Membrane-Bound Pyrophosphatase of *Thermotoga maritima* Requires Sodium for Activity†

Georgiy A. Belogurov,‡,§ Anssi M. Malinen,‡ Maria V. Turkina,§ Ulla Jalonen,‡ Kalle Rytkönen,‡ Alexander A. Baykov,*,§ and Reijo Lahti*,‡

Department of Biochemistry and Food Chemistry, University of Turku, FIN-20014 Turku, Finland, and A. N. Belozersky Institute of Physico-Chemical Biology and School of Chemistry, Moscow State University, Moscow 119899, Russia

Received July 22, 2004; Revised Manuscript Received September 23, 2004

ABSTRACT: Membrane-bound pyrophosphatase of the hyperthermophilic bacterium *Thermotoga maritima* (Tm-PPase), a homologue of H^+-translocating pyrophosphatase, was expressed in *Escherichia coli* and isolated as inner membrane vesicles. In contrast to all previously studied H^+-PPases, both native and recombinant Tm-PPases exhibited an absolute requirement for Na^+ but displayed the highest activity in the presence of millimolar levels of both Na^+ and K^+. Detergent-solubilized recombinant Tm-PPase was thermostable and retained the monovalent cation requirements of the membrane-embedded enzyme. Steady-state kinetic analysis of pyrophosphate hydrolysis by the wild-type enzyme suggested that two Na^+ binding sites and one K^+ binding site are involved in enzyme activation. The affinity of the site that binds Na^+ first is increased with increasing K^+ concentration. In contrast, only one Na^+ binding site (K^+-dependent) and one K^+ binding site were involved in activation of the $Asp^{703} \rightarrow$ Asn variant. Thus, Asp^{703} may form part of the K^+-independent Na^+ binding site. Unlike all other membrane and soluble PPases, Tm-PPase did not catalyze oxygen exchange between phosphate and water. However, solubilized Tm-PPase exhibited low but measurable PP_i-synthesizing activity, which also required Na^+ but was inhibited by K^+. These results demonstrate that *T. maritima* PPase belongs to a previously unknown subfamily of Na^+-dependent H^+-PPase homologues and may be an analogue of Na^+,K^+-ATPase.

The proton pumping pyrophosphatase (H^+-PPase)[1] is an integral membrane protein that utilizes the energy released by hydrolysis of pyrophosphate (PP_i) to transport protons across the membrane against the electrochemical potential gradient (*1*−*3*). In prokaryotic species, the H^+-PPase resides in the cytoplasmic membrane, whereas in eukaryotic species the enzyme is commonly found in membranes of organelles, such as vacuoles in plants (*4*) and acidocalcisomes in protozoa (*5*). A recent report indicates that the H^+-PPase of the bacterium *Agrobacterium tumefaciens* is located in acidocalcisome-like organelles (*6*). The substrate-binding domain always faces the cytoplasm, independent of H^+-PPase subcellular localization.

H^+-PPases represent a distinct class of ion translocases without sequence similarity to ubiquitous ATP-energized pumps, including the F-, V-, and P-type ATPases and the ABC transporters (*7*). Both PP_i-hydrolyzing and proton translocation activities are associated with a single 66−90 kDa polypeptide (*8*−*10*), which possibly forms a dimer (*11*, *12*). H^+-PPases act specifically on PP_i and display an obligate requirement for Mg^{2+}, which binds to and activates both the free enzyme and PP_i. Some H^+-PPases also require K^+ binding at the cytoplasmic side of the membrane (*2*, *13*). K^+-dependent and -independent enzymes form two independently evolving groups of H^+-PPases (*14*, *15*). A Lys residue is specifically conserved in the K^+-independent H^+-PPases. When this Lys is introduced into a K^+-dependent H^+-PPase, it abolishes K^+ dependence (*15*). Finally, a K^+ transporting function has been proposed for the K^+-dependent H^+-PPases in plant vacuoles (*16*), but this issue is controversial (*9*, *17*).

The hyperthermophilic bacterium *Thermotoga maritima* contains a membrane-bound PPase (Tm-PPase) that is homologous to H^+-PPases. This enzyme was previously expressed in the yeast *Saccharomyces cerevisiae* and reported to be K^+-dependent (*14*). Here we show that expression of Tm-PPase in *Escherichia coli* results in a markedly higher yield than in yeast, allowing a detailed characterization of this enzyme. We also show that, in contrast to all previously studied H^+-PPases, Tm-PPase has an absolute requirement for Na^+ and displays maximal activity in the presence of millimolar levels of both Na^+ and K^+. Finally, we used steady-state kinetic analysis of PP_i hydrolysis by Tm-PPase

† This work was supported by grants from the Academy of Finland (201611), the National Graduate School in Informational and Structural Biology, the Russian Foundation for Basic Research (03-04-48798), and the Ministry of Industry, Science and Technologies of the Russian Federation (1706-2003-4).

* To whom correspondence should be addressed. Reijo Lahti, tel. +358 2 3336845, fax +358 2 3336860, reijo.lahti@utu.fi or Alexander A. Baykov, tel. +7 095 9395541, fax +7 095 9393181, baykov@genebee.msu.su.

‡ University of Turku.

§ Moscow State University.

[1] Abbreviations: H^+-PPase, proton translocating inorganic pyrophosphatase; IMV, inner membrane vesicles; MOPS, 3-(*N*-morpholino)-propanesulfonic acid; PPase, pyrophosphatase; TMA, tetramethylammonium; Tm-PPase, *Thermotoga maritima* pyrophosphatase.

10.1021/bi048429g CCC: $30.25
Published on Web 01/15/2005

to estimate the number of alkali cation binding sites on the enzyme, and site-directed mutagenesis to clarify the role of two unique Asp residues in the alkali cation sensitivity of Tm-PPase.

MATERIALS AND METHODS

Materials. The following high purity reagents free of contaminating metal ions were obtained from commercial sources: MOPS (Sigma, USA; catalog no. M5162), TMA hydroxide pentahydrate (Fluka, Switzerland; catalog no. 87741), TMA chloride (Fluka, catalog no. 87718), potassium hydroxide (Fluka, catalog no. 60381), sodium hydroxide (Fluka, catalog no. 71695), potassium chloride (J. T. Baker, Holland; catalog no. 0208), sodium chloride (J. T. Baker, catalog no. 0277), and EGTA (Sigma, catalog no. E-0396). Tetramethylammonium (TMA) pyrophosphate was prepared by passing a solution of tetrasodium pyrophosphate through a column of Dowex 50W-X8 (Fluka) charged with TMA^+. The concentration of the resulting TMA_4PP_i solution was determined by measuring the amount of P_i after boiling in 1 M hydrochloric acid. Phosphoric acid (J. T.Baker, Holland), which was used as a source of phosphate, was diluted to 0.15 M, boiled for 3 h to hydrolyze contaminating PP_i, and adjusted to pH 7.5 with TMA hydroxide (TMAOH). ^{18}O-enriched (>98%) phosphate (Tris salt) was kindly donated by Dr. V. Kasho (University of California, Los Angeles).

Plasmid Construction. The Tm-PPase gene (GenBank accession number AE001702, bases 8378−10558; protein accession number AAD35267) (*18*) was amplified from *T. maritima* genomic DNA (DSMZ, Germany) by PCR using *Pfu*-Turbo DNA polymerase (Stratagene, USA). The primers employed incorporated artificial *Nde*I and *Hind*III restriction sites. The PCR product was digested with these restriction enzymes and was inserted into the multiple cloning site of pET36b(+) (Novagen, USA). The construct was further modified by replacing sequence AGAGGGG at positions 87 to 93 of the Tm-PPase gene with TGAAGGC. This silent mutation eliminated the Shine-Dalgarno-like sequence located upstream of the internal ATG codon. In addition, a second silent mutation was introduced by substituting sequence AGAAGACAGGCTCGA at positions 1732 to 1746 with CGTCGCCAGGCTCGC, thereby replacing the tandem of rare arginine codons with more frequently used codons. The resulting construct was used for wild-type Tm-PPase expression or as a template for mutagenesis of Asp^{190} and Asp^{703}. Mutagenesis was performed by an overlapping or inverse PCR (*19*). Tm-PPase-encoding regions of the constructs were sequenced to confirm the presence of the required mutations and/or the absence of secondary substitutions.

Tm-PPase Expression. Tm-PPase was expressed in *E. coli* C41(DE3) cells (*20*) bearing the pET36b(+) vector, which contains the Tm-PPase gene under control of the T7/lac promoter, and an additional pAYCA-RIL plasmid extracted from BL21(DE3)-RIL (Stratagene, USA). The latter plasmid supplied tRNAs that recognize the AGA/AGG, AUA, and CUA codons, which are common in the Tm-PPase gene but rare in *E. coli*, thereby preventing the depletion of the *E. coli* tRNA pool. Cells were grown at 37 °C with shaking at 250 rpm in a medium containing 24 g/L yeast extract, 10 g/L trypton, 2.5 g/L KCl, 2.5 g/L NaCl, and 0.6 g/L NaOH supplemented with 30 μg/mL kanamycin and 30 μg/mL chloramphenicol. A 5 mL culture was grown for 4 h and transferred to 1 L of prewarmed medium. Cells were grown to an A_{600} of 0.8 (~3 h), induced with 0.1 mM isopropyl-β-D-thiogalactopyranoside for 4.5 h, and harvested by centrifugation at 2700*g* for 15 min at 4 °C. The cells were washed three times with 10 mM MOPS-TMAOH, pH 7.2 supplemented with 10% glycerol, frozen in liquid nitrogen, and stored at −70 °C until use.

Isolation of E. coli Inner Membrane Vesicles (IMV). The cell pellet (8 g wet weight) was resuspended in 30 mL of buffer A (10 mM MOPS-TMAOH, pH 7.2, 0.15 M sucrose, 1 mM $MgCl_2$, 5 mM dithiothreitol, 50 μM EGTA) supplemented with DNase I (20 μg/mL) and disrupted by a single passage through a French pressure cell at 14 000 psi (96.5 MPa). Unbroken cells and cell debris were removed by centrifugation at 38000*g* for 30 min at 4 °C. The supernatant was transferred to an ultracentrifuge bottle, underlayered with 4 mL of buffer A supplemented with 0.75 M sucrose, and centrifuged at 150000*g* for 3 h at 4 °C. The IMV suspension (3.5 mL) was withdrawn from the bottom of the bottle, diluted with buffer A to 20 mL, and the ultracentrifugation step was repeated. The purified IMV suspension was frozen in liquid nitrogen and stored at −70 °C until use.

Solubilization and Purification of Tm-PPase. All steps were performed at 4 °C. The cell pellet obtained from 4 L of cell culture was resuspended in 1 L of 10 mM Tris-HCl, pH 7.5, containing 5 mM $MgCl_2$ and 150 mM KCl. The resuspended cell pellet was sedimented at 2700*g* for 20 min and then resuspended in 30 mM Tris-HCl, pH 7.5 containing 5 mM $MgCl_2$, 100 mM KCl, and 0.5 mM EDTA. Cells were disrupted by sonication for 1 min at 22 kHz in an ice−water bath using a 100 W ultrasonic disintegrator (MSE Ltd., UK) with a microtip. Unbroken cells and cell debris were removed by centrifugation at 17000*g* for 5 min, and the membrane fraction was harvested by centrifugation at 150000*g* for 1 h. The resulting pellet was resuspended in 3 mL of sonication buffer and sedimented as above. This pellet was solubilized in 50 mM Tris-HCl, pH 8.4, containing 1.5% MEGA9 (Sigma), 0.5% sodium cholate, 25% ethelene glycol, 0.75 M $MgCl_2$, and 0.2 mM dithiothreitol (0.2 to 0.5 mL buffer per mg protein) (*8*). After incubating the sample for 1 h on ice with gentle mixing, the suspension was centrifuged at 17000*g* for 1 h. The supernatant was mixed with saturated $(NH_4)_2SO_4$ solution to a final concentration of 2.5 M $(NH_4)_2SO_4$, incubated on ice for 1 h, and centrifuged at 7500*g* for 30 min. The supernatant was applied to a 14-mL column of phenyl Sepharose (Pharmacia-LKB, Sweden) equilibrated with 20 mM Tris-HCl, pH 7.5, containing 2.5 M $(NH_4)_2SO_4$, 1 mM $MgCl_2$, 0.2 mM EDTA, and 0.2 mM dithiothreitol. The column was washed with 14 mL of the same buffer and then with 80 mL of the same buffer without $(NH_4)_2SO_4$. Tm-PPase was eluted with 20 mM Tris-HCl, pH 7.5 containing 1.5% dodecyl maltoside (Anatrace, USA), 1 mM $MgCl_2$, 0.2 mM EDTA, and 0.2 mM dithiothreitol. The active fractions contained 17 mg of protein with a specific activity of 4.5 μmol min^{-1} mg^{-1}. They were frozen in liquid nitrogen and stored at −50 °C.

Isolation of T. maritima Membrane Vesicles. T. maritima (DSM 3109) was grown anaerobically in a 10 L fermentor under a nitrogen flow at 2 L/min for 24 h as described previously (*21*). The cells were harvested by centrifugation

at 10000*g* for 15 min at 4 °C, resuspended in 500 mL of 10 mM MOPS-TMAOH, pH 7.2, and collected by centrifugation at 10000*g* for 15 min at 4 °C. Finally, the cells were washed three times with 10 mM MOPS-TMAOH, pH 7.2 supplemented with 10% glycerol. The washed cell pellet (~3 g) was resuspended in 5 mL of 10 mM MOPS-TMAOH buffer, pH 7.2, containing 5 mM $MgCl_2$, 50 μM EGTA, 10% glycerol, and disrupted by sonication for 2 min at an operating frequency of 20 kHz and a 9-μm amplitude in an ice−water bath using a 100 W ultrasonic disintegrator (MSE Ltd.) with a microtip. Unbroken cells and cell debris were removed by centrifugation at 20000*g* for 2 min at 4 °C. The supernatant was diluted 20-fold with buffer A, and the membrane fraction was harvested by centrifugation at 150000*g* for 1 h. The resulting pellet was resuspended in 3 mL of buffer A, homogenized by brief sonication (30 s) as described above, frozen in liquid nitrogen, and stored at −70 °C until use.

PP_i Hydrolysis Measurements. PP_i hydrolysis was assayed by continuously recording P_i liberation with an automatic P_i analyzer (*22*) at 40 °C. The reactions were performed in an initial volume of 25 mL containing 100 mM MOPS-TMAOH buffer, pH 7.2 (measured at 25 °C), 5.26 mM $MgCl_2$ (5 mM free Mg^{2+}), 160 μM TMA_4PP_i, 50 μM EGTA and 5 to 50 μL of IMV suspension or purified Tm-PPase solution. The IMV were preincubated in the reaction medium for 1 min, the reaction was initiated by the addition of TMA_4PP_i, and P_i liberation was monitored for 3 min. The desired concentrations of K^+ and Na^+ in the reaction medium were achieved by addition of KCl and NaCl, respectively, or by substituting MOPS-KOH and MOPS-NaOH buffers, respectively, for MOPS-TMAOH buffer. When below 0.2 mM, the concentrations of Na^+ and K^+ in assay media were determined by atomic absorption spectrometry (SpectrAA-300, Varian Techtron, Australia). In some experiments, ionic strength and chloride concentration were maintained at 0.22 and 0.1 M, respectively, by adding TMA chloride. Data obtained with and without TMA chloride were superimposable, suggesting that ionic strength and chloride concentration do not significantly affect enzyme activity. Similarly, the dependencies of PPase activity on the Na^+ concentration were identical when measured at 160 and 80 μM of PP_i. This implies that the enzymes were likely saturated with substrate in our experiments.

Measurements of PP_i Synthesis. PP_i synthesis was assayed by an enzyme-coupled procedure (*23*, *24*) using ATP-sulfurylase to convert formed PP_i into ATP combined with luciferase to monitor ATP formation. The assay mixture contained 32 mM TMA-P_i (2 mM MgP_i complex), 2.5 mM $MgCl_2$ (0.5 mM free Mg^{2+}), 0.13 mg/mL purified Tm-PPase, 0.7 U/mL ATP-sulfurylase (Sigma), 10 μM adenosine-5′-phosphosulfate, and 0.1 M MOPS-TMAOH buffer in a total volume of 0.2 mL. Care was taken to ensure that the ATP-sulfurylase concentration was sufficiently high so that PP_i conversion into ATP proceeded at least 20 times faster than PP_i formation. The reaction was initiated by adding P_i and carried out at 40 °C for 10 min. Aliquots (30 μL) were withdrawn at various times, quenched with 30 μL of 1 M trifluoroacetic acid, incubated for 3 to 4 min at room temperature, and neutralized with 30 μL of 1.5 M Tris. The ATP formed was assayed by adding 10 μL of the resulting mixture to 0.2 mL of 0.2 M Tris-HCl, pH 8.0 containing 5 μL of luciferin/luciferase solution (Sigma ATP assay mix, catalog No. FL-ASC, reconstituted with 5 mL of water) and measuring the resulting luminescence with an LKB 1250 luminometer.

Scheme 1: Na^+ Binding to Tm-PPase at Fixed K^+ Concentrations

A. Wild type and D190A Variant

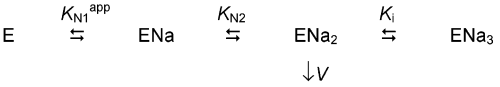

B. D703N and D190A/D703N Variants

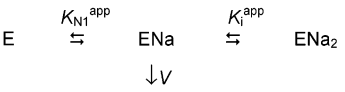

P_i-Water Oxygen Exchange Measurements. Purified Tm-PPase (0.21 mg/mL) was incubated for 1 h at 40 °C with 2 mM [^{18}O]P_i, 5 or 0.5 mM $MgCl_2$, 0.1 M MOPS-TMAOH buffer, and various concentrations of NaCl and KCl. The amount of ^{18}O in P_i was measured with an electrospray mass spectrometer as described previously (*25*).

Sodium Dodecyl Sulfate-Polyacrylamide Gel Electrophoresis (SDS−PAGE) and Protein Quantitation. Electrophoresis was performed in 12% gels containing 0.1% SDS (*26*). Prior to electrophoresis, IMV (~20 mg of protein/mL according to the Bradford assay (*27*)) were solubilized by mixing with two volumes of cold 25 mM Tricine-KOH buffer, pH 8.1 containing 5 mM $MgCl_2$, 75 mM KCl, 5 mM dithiothreitol and 2% *n*-dodecyl-β-D-maltoside. The mixture was allowed to stand on ice for 5 h and incubated for 10 min at 75 °C. Denatured proteins were removed by centrifugation at 20000*g* for 20 min. More than 95% of the solubilized PPase activity was retained in the supernatant. The supernatant was diluted 3-fold with 125 mM Tris-HCl buffer, pH 6.8, containing 20% glycerol, 300 mM dithiothreitol, and 2.5% sodium dodecyl sulfate, incubated for 5 min at 95 °C, and a 10 μL sample was loaded onto the gel. The gels were stained using a Biosafe Coomassie kit (Bio-Rad, California, USA) and scanned using an Umax Astra 3450 scanner in transmission mode. The protein content of the Tm-PPase bands (0.4−0.6 μg) were estimated by ImageJ, version 1.3 (http://rsb.info.nih.gov/ij/) using bands containing 0.2, 0.5, and 0.8 μg of bovine serum albumin as standards.

Calculation and Data Analysis. The dependence of the PP_i hydrolysis rate on the Na^+ concentration at fixed K^+ concentration can be described by Scheme 1, where E represents the enzyme−PP_i−Mg^{2+} complex, Na is Na^+, K_{N1}^{app}, K_{N2}, and K_i^{app} are Na^+ binding constants, V is the Na^+ concentration-independent catalytic activity, and v_0 is the background activity due to contaminating *E. coli* PPase. For the wild-type enzyme and the D190A variant, two activating Na^+ ions are bound (Scheme 1A), whereas for the D703N and D190A/D703N variants, only one activating Na^+ ion is bound (Scheme 1B). In both cases, only one inhibiting Na^+ ion is bound, and its binding is described by the dissociation constant K_i or K_i^{app}. Scheme 1 assumes that the enzyme species are in equilibrium with each other. The parameters in Scheme 1A,B were determined by fitting the rate data to eqs 1A or 1B, respectively, using SCIENTIST software (MicroMath, Missouri, USA). Rates (v) were weighted

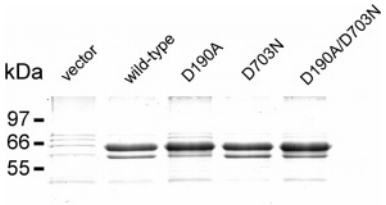

FIGURE 1: Heat-resistant proteins in IMV from C41(DE3) cells expressing wild-type and mutated Tm-PPases or transformed with an empty vector. IMV were solubilized with *n*-dodecyl-*β*-D-maltoside and were treated for 10 min at 75 °C. Denatured proteins were removed by centrifugation, and the supernatant was subjected to SDS−PAGE.

according to $1/v$.

$$v = V/(1 + K_{N2}/[Na] + K_{N1}^{app}K_{N2}/[Na]^2 + [Na]/K_i) + v_0 \quad (1A)$$

$$v = V/(1 + K_{N1}^{app}/[Na] + [Na]/K_i^{app}) + v_0 \quad (1B)$$

RESULTS

Heterologous Expression of Tm-PPase in E. coli. We expressed Tm-PPase in *E. coli* C41(DE3) using the method previously established for *Rhodospirillum rubrum* H^+-PPase (*28*). IMV prepared from C41(DE3) cells expressing Tm-PPase were solubilized in *n*-dodecyl-*β*-D-maltoside, heat-treated, and analyzed by SDS−PAGE. This analysis revealed an intense 66-kDa band (Figure 1) that was absent in IMV from C41(DE3) cells transformed with empty pET36b(+). Although a molecular mass of 73 kDa is predicted from the amino acid sequence of Tm-PPase, it is likely that the 66-kDa band is the full-length enzyme because many reports have shown similar anomalous mobilities for H^+-PPases on SDS−PAGE (*8*, *15*, *28*).

Because *E. coli* IMV lack endogenous membrane PPases, PP_i hydrolysis by Tm-PPase could be assayed directly in the IMV. Although the optimal temperature range for the growth of *T. maritima* is 75 to 85 °C, PP_i hydrolysis by Tm-PPase in *E. coli* IMV was measured at 40 °C to maintain the natural lipid bilayer environment. In the presence of 25 mM Na^+ and 50 mM K^+, the *E. coli* IMV containing Tm-PPase displayed a salt wash-resistant, Mg^{2+}-dependent PPase activity. In addition, the PPase had the characteristics of H^+-PPase (*29*), including hypersensitivity to the H^+-PPase inhibitor, aminomethylenediphosphonate (>95% inhibition at 20 μM), and low sensitivity to the soluble PPase inhibitor, fluoride (5% inhibition by 0.25 mM). The specific activity of the IMV PPase was 0.4 μmol min^{-1} mg^{-1} total IMV protein (21 μmol min^{-1} mg^{-1} Tm-PPase protein). In contrast, the PPase activity of the control IMV lacking the Tm-PPase was 40-fold lower. Because this residual activity was salt-washable and entirely fluoride-sensitive (>95% inhibition by 0.25 mM), it appeared to be due to contaminating soluble *E. coli* PPase.

Tm-PPase could be extracted from IMV membrane using the nonionic detergent MEGA9 without any loss in activity. Thereafter, it could be purified 11-fold by a single step of phenyl-Sepharose chromatography. The purified enzyme retained the characteristics of the IMV activity and was stable in solution for at least one week at 4 °C.

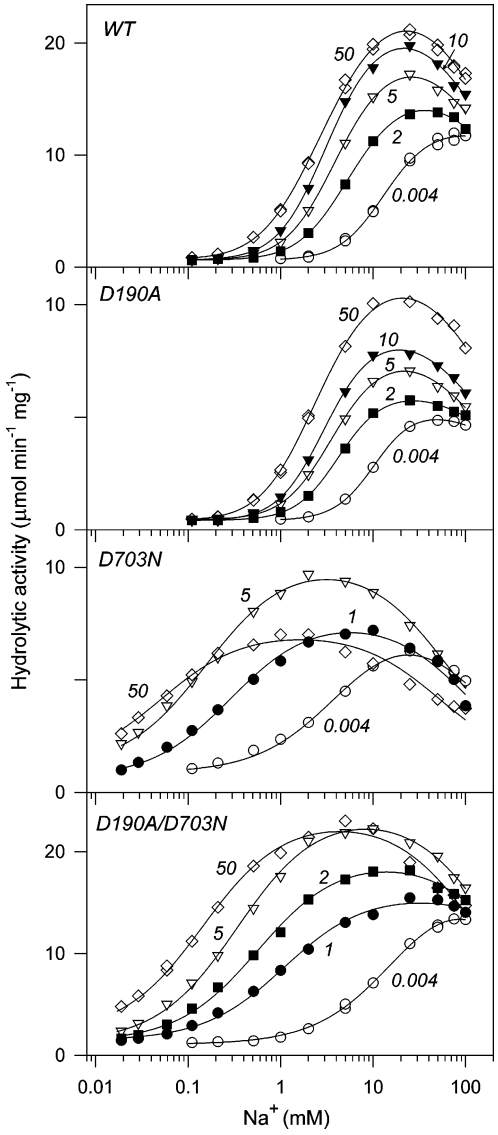

FIGURE 2: Na^+ dependence of the rate of PP_i hydrolysis for the wild-type and variant IMV Tm-PPases at fixed K^+ concentrations (shown on the curves in mM). Lines were drawn according to eq 1A for the wild-type and D190A enzymes and eq 1B for the D703N and D190A/D703N enzymes. The values of activity are per mg of Tm-PPase protein.

Tm-PPase Requires Na^+ for Activity. In a K^+-free (<5 μM K^+) medium, Tm-PPase activity increased with increasing concentration of Na^+ and leveled off at the upper limits of the examined Na^+ concentration range (Figure 2, panel marked WT). Increasing the K^+ concentration progressively shifted the activity optimum toward lower Na^+ concentrations and increased the maximum activity. In the presence of 5 mM Na^+, the activity hyperbolically increased with increasing K^+ concentration (Figure 3). Similar hyperbolic dependencies were observed at fixed Na^+ concentrations of 2, 10, and 50 mM (data not shown). However, in a Na^+-free (<10 μM Na^+) medium, there was no difference between the Tm-PPase and background activities (0.5 μmol min^{-1} mg^{-1}) over the whole K^+ concentration range examined. These data indicated that Tm-PPase absolutely requires Na^+ for activity, whereas both Na^+ and K^+ are needed for maximal activity. Importantly, detergent-solubilized, purified recombinant Tm-PPase and Tm-PPase in membrane vesicles from *T. maritima* (activities measured at 40 and 80 °C,

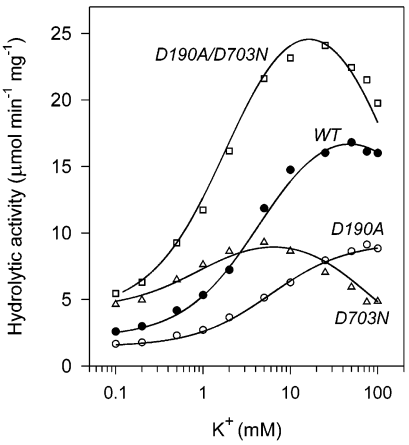

FIGURE 3: K^+ dependence of the rate of PP_i hydrolysis for the wild-type and variant IMV Tm-PPases in the presence of 5 mM Na^+. Lines were drawn according to eq 1B with [K^+] substituting for [Na^+].

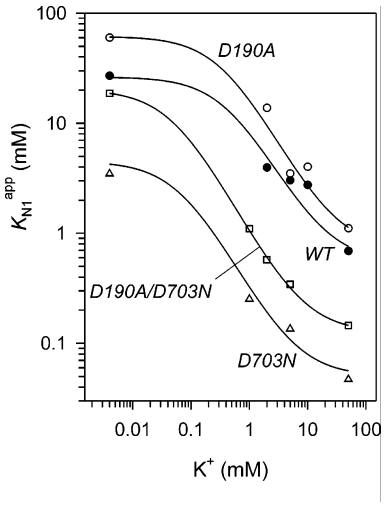

FIGURE 4: K^+ dependence of K_{N1}^{app} for the wild-type and variant IMV Tm-PPases as estimated from the data in Figure 2. Lines were drawn according to eq 2 using the parameter values from Table 1.

respectively; data not shown) had similar requirements for alkali cations.

Interestingly, Li^+ can substitute for Na^+ as activator of Tm-PPase in IMV. In the absence of K^+, the Li^+ and Na^+ dose-dependencies were superimposable, and they were similarly shifted toward lower activator concentrations with increasing K^+ concentrations (data not shown). However, they differed in that K^+ did not increase the maximal activity of the Li^+-activated enzyme. As a result, in the presence of K^+, Li^+ was a less potent activator than Na^+.

The Na^+ dependencies of wild-type Tm-PPase shown in Figure 2 were described well by eq 1A for two activating Na^+ sites, whereas fitting the data to eq 1B for one activating Na^+ site resulted in a poor fit; the sum of the squares of residuals increased by a factor of 2.5 to 8, and systematic deviations were observed in the latter case. This indicated that Tm-PPase has at least two binding sites for activating Na^+ ion. The value of K_{N1}^{app} obtained from these fittings decreased approximately 40-fold as the K^+ concentration increased, eventually reaching a constant value (Figure 4), whereas the value of K_{N2} remained constant (3 ± 1 mM) within the error of determination. Thus, K^+ greatly stimulates Na^+ binding to one of the two activating Na^+ sites in Tm-PPase. The value of K_i, which was quite high at low [K^+], was independent of [K^+] within the error of determination. The mean value of K_i was 200 ± 40 mM for the wild-type enzyme. Because of the inhibition, the activity could not approach its limiting value, V. However, because K_i significantly exceeded both K_{N1}^{app} and K_{N2}, the maximum value of v differed from V by only 10 to 20%. It should be noted that Scheme 1A and eq 1A assume that ENa_3 has no activity. This assumption could not be directly tested because of the weakness of the inhibition, but the conclusions are the same regardless of whether this enzyme species has activity.

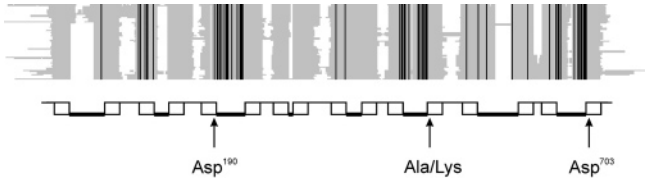

FIGURE 5: Alignment of nonredundant H^+-PPase sequences. The 48 sequences used are from Belogurov and Lahti (*15*). Conserved and nonconserved amino acid positions are shaded in black and gray, respectively. The tentative transmembrane topology generated by HMMTOP (*30*) for Tm-PPase is indicated below the alignment. This predicted toplogy of Tm-PPase is compatible with experimentally determined topology of *Streptomyces coelicolor* H^+-PPase (*31*). Transmembrane segments are drawn as rectangles, periplasmic loops are drawn as lines, and cytoplasmic loops are drawn as bold lines. Arrows indicate the positions of Asp^{190} and Asp^{703} as well as an Ala/Lys position where K^+-dependent and K^+-independent H^+-PPases differ (*15*).

Effects of Asp^{190} → Ala and Asp^{703} → Asn Substitutions. A requirement for Na^+ is unique to Tm-PPase. We noticed that Tm-PPase also differs from other H^+-PPases because it possesses Asp^{190} and Asp^{703}, which are located in highly conserved regions at the predicted cytoplasm−membrane interface (Figure 5). To determine the effects of these residues on the requirement for Na^+, we replaced Asp^{190} with Ala and Asp^{703} with Asn either separately or in combination. These substitutes were chosen from the residues at the same positions in phylogenetically related H^+-PPases that do not require Na^+. The resulting D190A, D703N, and D190A/D703N variants were expressed in *E. coli* C41(DE3). On the basis of the intensities of the corresponding bands on SDS−PAGE (Figure 1), these proteins were expressed with similar yields as the wild-type enzyme.

All three variants required Na^+ for activity and both Na^+ and K^+ for maximal activity. The Na^+ dose dependencies of the PPase activity for the D190A variant closely resembled those of the wild-type enzyme and also obeyed eq 1A (Figure 2, D190A). In addition, the values for K_{N1}^{app} (Figure 4), K_{N2}, and K_i^{app} were similar to those for the wild-type enzyme, and the latter parameter was also independent of [K^+]. In contrast, the D703N variant exhibited a much lower slope on the rate vs [Na^+] plot than the wild-type enzyme at all of the K^+ concentrations examined. Fitting eq 1A to the data in Figure 2 for this variant resulted in zero or even slightly negative values for K_{N1}^{app}. Therefore, eq 1B was used, assuming one activating Na^+ binding site (Scheme 1B). The K_{N1}^{app} values thus generated were an order of magnitude lower for this variant than for the wild-type enzyme but exhibited the same dependence on [K^+] (Figure 4); specifically, K^+ also stimulated Na^+ binding. Furthermore, the K_i^{app} values for this variant progressively decreased from

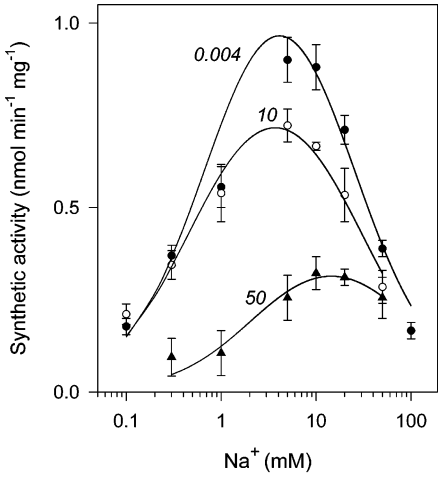

FIGURE 6: Na^+ dependence of the rate of PP_i synthesis by purified wild-type Tm-PPase at fixed K^+ concentrations (shown on the curves in mM). The values of activity are per mg of total protein.

170 to 60 mM when the K^+ concentration was increased from 0.004 to 50 mM. Activation of the D190A/D703N variant by alkali cations was similar to the D703N variant, but the maximum was shifted to 2-fold higher Na^+ and K^+ concentrations (Figures 2 and 3). These results demonstrated that Asp^{703} but not Asp^{190} is involved in Na^+ activation of Tm-PPase and that Asp^{703} replacement silences the K^+-independent activating Na^+-binding site.

The K^+ dose dependence of the PPase activity at fixed Na^+ concentration for the D190A variant also closely resembled that for the wild-type enzyme (Figure 3). For both D703N variants, these dependencies were distinctly bell-shaped with the maximum at about 10 mM K^+ concentration.

Na^+,K^+ Requirements for PP_i Synthesis. Initial rates of PP_i synthesis by purified Tm-PPase were measured by incubating PP_i-free P_i with Tm-PPase in the presence of ATP-sulfurylase, which rapidly and quantitatively converts the formed PP_i into ATP (*23*, *32*). In this way, the steady-state PP_i concentration is kept far below its equilibrium level, which was as low as 0.27 μM under the conditions used in the present work (0.5 mM Mg^{2+}, 32 mM total P_i, pH 7.5) (*33*). The accumulated ATP was then measured with a sensitive luciferase assay. This approach, employed in previous studies of soluble PPases (*24*, *25*, *34*, *35*), could also be applied to purified Tm-PPase. However, the synthesizing activity of IMV Tm-PPase could not be assayed by this method because of high ATPase activity present in IMV membranes.

PP_i synthesis could not be detected (<0.1 nmol min^{-1} mg^{-1}) in the absence of Na^+ over a $[K^+]$ range from 0.3 to 50 mM. In the presence of Na^+, the rate was low but measurable (Figure 6). The rate vs $[Na^+]$ profiles were bell-shaped, indicating that Na^+ both activates and inhibits PP_i synthesis, as it does for PP_i hydrolysis. Because of large data scatter, the stoichiometry of Na^+ participation could not be established, but at least one activating and one inhibiting Na^+ ion is involved. Surprisingly, K^+ inhibited Na^+-dependent PP_i synthesis.

All PPases studied so far catalyze oxygen exchange between P_i and water at a rate comparable to that of PP_i hydrolysis. This reaction occurs as a reversal of PP_i synthesis on the enzyme (*36*). Examples of H^+-PPases catalyzing rapid oxygen exchange include those from the bacterium *Rhodospirillum rubrum* (*37*) and the plant *Vigna radiata* (*38*). Surprisingly, oxygen exchange between $[^{18}O]P_i$ and $[^{16}O]$water was not observed (<5 nmol min^{-1} mg^{-1}) with IMV or purified Tm-PPase either in the absence of alkali metal ions or in the presence of 10 mM Na^+, 50 mM K^+, or a combination of both Na^+ and K^+.

Scheme 2: Na^+ and K^+ Binding to Tm-PPase

A. Wild type and D190A Variant

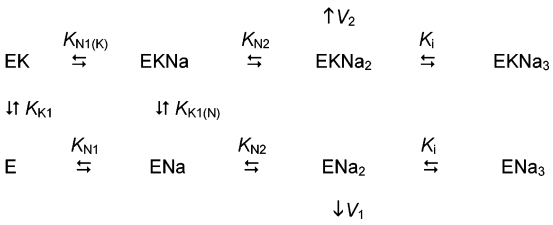

B. D703N and D190A/D703N Variants

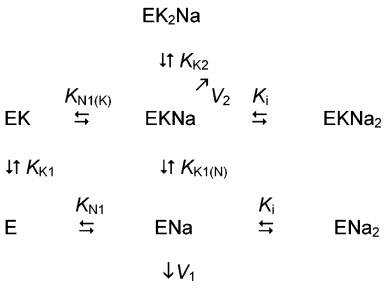

DISCUSSION

The present results show that Tm-PPase is the first Na^+-dependent PPase and is, therefore, distinct from conventional K^+-dependent H^+-PPases that can employ Na^+ as an alternative activator. For example, although Na^+ can substitute for K^+ as activator of H^+-PPase from *Carboxydothermus hydrogenoformans*, K^+ alone is sufficient for activation, and activation by Na^+ is not observed at saturating concentrations of K^+ (Belogurov, G. A., unpublished results). In contrast, Tm-PPase absolutely requires Na^+ for activity both in the presence and absence of K^+. Importantly, the Na^+ dependence of recombinant Tm-PPase is not an artifact of heterologous expression in *E. coli* because the PPase activity in native *T. maritima* membranes is also Na^+-dependent.

Kinetic Scheme of Na^+ and K^+ Activation. The effects of Na^+ and K^+ on Tm-PPase activity can be interpreted by means of the simple kinetic models shown in Scheme 2. These are an extension of the models in Scheme 1 and involve two similar, parallel routes: one for K^+-free enzyme and the other for K^+-bound enzyme. The model in Scheme 2A implies the presence of four binding sites for alkali cations in the wild-type and D190A enzymes, including two activating and one inhibitory site for Na^+ and one activating site for K^+ ($V_2 > V_1$). In the D703 variants, one activating site is lost, but one inhibitory site for K^+ is gained (Scheme 2B). The latter explains the observed dependence of K_i^{app} in Scheme 1B on $[K^+]$ and the decrease in activity at high $[K^+]$ in Figure 3. Binding of the inhibitory K^+ ion also explains the potentiation of inhibition by excess Na^+ observed in Figure 2 for both D703N variants. The latter effect suggests that, as shown in Scheme 2B, the inhibiting K^+ ion binds to

Table 1: Parameters for Schemes 2A and 2B

parameter	wild type	wild type[a]	D190A	D703N	D190A/D703N
K_{N1} (mM)	26 ± 10	70 ± 40	62 ± 24	4.5 ± 1.7	20 ± 1
$K_{N1(K)}$ (mM)	0.5 ± 0.3	1.0 ± 0.3	0.7 ± 0.3	0.05 ± 0.02	0.13 ± 0.01
K_{N2} (mM)	3 ± 1	3 ± 1	1.8 ± 0.4		
K_{K1} (mM)	19 ± 15	9 ± 3	30 ± 20	6 ± 4	7.9 ± 0.9
$K_{K1(N)}$ (mM)	0.4 ± 0.2	0.13 ± 0.06	0.34 ± 0.19	0.066 ± 0.038	0.049 ± 0.005
K_i (mM)	200 ± 40	200 ± 70	210 ± 60	170 ± 30	400 ± 100
K_{K2} (mM)				70 ± 10	240 ± 30
V_1 (μmol min^{-1} mg^{-1})[b]	13 ± 1	3.0 ± 0.2	5.2 ± 0.4	7.0 ± 0.3	17.5 ± 0.8
V_2 (μmol min^{-1} mg^{-1})[b]	20 ± 1	4.5 ± 0.3	10.0 ± 0.4	9.7 ± 0.4	27 ± 1

[a] Solubilized and partially purified wild-type Tm-PPase. [b] Activity of IMV is in terms of Tm-PPase protein, as estimated from SDS−PAGE, and activity of purified enzyme is in terms of total protein present in the preparation.

the enzyme species containing the full complement of activating ions (EKNa), although weaker binding to $EKNa_2$ and EK cannot be excluded. The binding constant for the first activating Na^+ ion to bind is assumed to be K^+-dependent ($K_{N1} \neq K_{N1(K)}$) in all enzymes, whereas the binding constant for the second activating Na^+ ion in the wild-type and D190A enzymes (K_{N2}) and for the inhibiting Na^+ ion in all enzymes (K_i) is assumed to be K^+-independent.

In terms of Scheme 2A,B, the dependence of K_{N1}^{app} on $[K^+]$ is given by eq 2. Fitting this equation to the data in Figure 4 allowed evaluation of K_{N1} and the two K^+ binding constants, K_{K1} and $K_{K1(N)}$. The value of $K_{N1(K)}$ could then be calculated as $K_{N1}K_{K1(N)}/K_{K1}$. The values of V_1 and V_2 could be approximated using the values of V estimated at 0.004 mM and optimal K^+ concentrations, respectively. Finally, the value of K_{K2} for the D703N variants was determined by fitting an equation analogous to eq 1B to the data in Figure 3 because the Na^+ and K^+ concentrations used were nearly saturating with respect to the activating cation-binding sites. The values of all parameters estimated in this way are summarized in Table 1, and they indicate that the effect of K^+ on wild-type Tm-PPase activity is 2-fold: it markedly increases enzyme affinity for Na^+ and it slightly increases the maximal activity.

$$K_{N1}^{app} = K_{N1}(1 + [K]/K_{K1})/(1 + [K]/K_{K1(N)}) \qquad (2)$$

According to Scheme 2, Na^+ is an essential activator and K^+ is a modulator of Tm-PPase activity. Because the cytosol contains ~100 mM K^+, Tm-PPase is expected to always be saturated with K^+. In contrast, the cytosolic Na^+ concentration may be well below 50 mM in *T. maritima* exposed to ~0.5 M Na^+ in seawater (*39*) because bacteria usually keep an internal $[Na^+]$ at least 10-fold lower than the external $[Na^+]$ (*40*−*44*). Therefore changes in cytosolic $[Na^+]$ may regulate Tm-PPase activity. Interestingly, K^+ activates PP_i hydrolysis by TM-PPase but inhibits PP_i synthesis. This indicates that K^+ binding may be essential to shift the enzyme activity toward PP_i hydrolysis under energized conditions.

Given the high affinity of Tm-PPase and especially of the D703N and D190A/D703N variants for Na^+, the Na^+ requirement of H^+-PPase homologues can be easily overlooked unless special precautions are taken. Indeed, these variants are fully activated at 0.5 to 1 mM Na^+, which is commonly present in biochemical experiments due to reagent contamination and cation leakage from glassware. In fact, the Na^+ requirement of wild-type Tm-PPase was not detected in its initial characterization (*14*), presumably due to employment of Na_4PP_i in hydrolysis studies. By using a Na^+-free system, we have determined that the K^+-dependent H^+-PPase from *C. hydrogenoformans* (*15*) and K^+-independent enzymes from *R. rubrum* (GenBank accession number AAC38615) and *Pyrobaculum aerophilum* (GenBank accession number AAF01029) are Na^+-independent. However, more enzymes, including those from plant vacuoles and protozoan acidocalcisomes, must be studied to determine the prevalence of Na^+ dependence among H^+-PPase homologues.

Possible Role of Asp[703]. In terms of Scheme 2, the most noticeable effects of the D703N substitution are to silence one activating Na^+ binding site, to increase the affinity of the remaining activating Na^+ binding site, and to generate one inhibitory K^+ binding site. One possible explanation is that the D703N substitution converted the activating Na^+ binding site to an inhibitory K^+ binding site. The effect of the D703N substitution on activating K^+ binding was moderate (a 3−7-fold decrease in K_{K1} and $K_{K1(N)}$; Table 1). Overall, the effects of the D703N mutation suggest that Asp^{703} directly participates in Na^+ binding. However, this residue is not the sole determinant of Na^+ dependence because the D703N variant still absolutely requires Na^+ for activity.

In contrast to the effects of the D703N substitution, the effects of the D190A mutation were quite small, indicating that Asp^{190} probably does not interact with alkali cations in Tm-PPase. Interestingly, whereas both the D190A and D703N variants had 2-fold lower PPase activities than the wild-type enzyme, the double mutant regained wild-type activity. This compensatory effect suggests that Asp^{190} and Asp^{703} are close to each other in the Tm-PPase structure.

Alternative Activities of Tm-PPase. Like any catalyst, Tm-PPase is able to catalyze the reverse reaction, PP_i synthesis (Figure 6). This spontaneous reaction establishes an equilibrium between PP_i and P_i, and is distinct from the energy-driven PP_i synthesis in membrane systems, which can raise the level of PP_i above this equilibrium. Tm-PPase is, however, unique because its synthesizing activity is very low (0.9 nmol min^{-1} mg^{-1}), representing only 0.02% of its hydrolytic activity (4.5 μmol min^{-1} mg^{-1}). In comparison, for other PPases, this percentage is typically around 1%, although a value as high as 16% has been reported for rat liver PPase (*35*). For *R. rubrum* PPase, the only H^+-PPase for which PP_i synthesis was measured under nonenergized conditions (*28*), this value is 0.6%. This synthesis of PP_i by a PPase involves three steps: P_i binding to the active site, formation of an enzyme-bound PP_i, and release of PP_i into

solution. The other typical PPase reaction, P_i−water oxygen exchange, occurs by P_i binding to the active site, formation of enzyme-bound PP_i, hydrolysis of PP_i, and release of P_i into solution (*36*). For Tm-PPase, this reaction is also quite slow (<5 nmol min^{-1} mg^{-1}). Thus, the first two steps of P_i−water oxygen exchange are the same as in PP_i synthesis and may include a common rate-determining step. The third and the fourth steps of oxygen exchange cannot be slow because they are also partial reactions of the much faster PP_i hydrolysis. Pre-steady-state kinetic analysis of Tm-PPase catalysis will help to identify the rate-determining step with more certainty and will also establish its Na^+ and K^+ requirements.

Interestingly, both the Na^+ and K^+ binding sites of Tm-PPase, which likely occur in the vicinity of Asp^{703} and the Ala/Lys position (*15*), respectively, map to the cytoplasm−membrane interface in a computer-generated topological model (Figure 5) (*30*, *31*). This observation raises the intriguing possibility that these ions are translocated by the enzyme or were translocated by its extinct ancestor. The slowness of PP_i synthesis and P_i−water oxygen exchange may therefore indicate tight coupling between these reactions and ion transport. However, experiments to test the possibility that Tm-PPase translocates any combination of H^+, Na^+, and K^+ were complicated by the oxygen sensitivity of *T. maritima* membranes and the high passive ion conductance of the *E. coli* IMV membrane at temperatures above 30 °C where Tm-PPase is sufficiently active. The investigation of ion transport by Na^+,K^+-dependent H^+-PPase may therefore require characterization of its mesophilic homologue.

ACKNOWLEDGMENT

We thank Dr. J. E. Walker for providing the *E. coli* C41(DE3) strain.

REFERENCES

1. Baltscheffsky, M., Schultz, A., and Baltscheffsky, H. (1999) H^+-proton-pumping inorganic pyrophosphatase: a tightly membrane-bound family, *FEBS Lett. 452*, 121−127.
2. Maeshima, M. (2000) Vacuolar H^+-pyrophosphatase, *Biochim. Biophys. Acta 1465*, 37−51.
3. Drozdowicz, Y. M., and Rea, P. A. (2001) Vacuolar H^+-pyrophosphatases: from the evolutionary backwaters into the mainstream, *Trends Plant Sci. 6*, 206−211.
4. Rea, P. A., and Poole, R. J. (1993) Vacuolar H^+-Translocating Pyrophosphatase, *Annu. Rev. Plant. Physiol. Plant Mol. Biol. 44*, 157−180.
5. Docampo, R., and Moreno, S. N. (2001) The acidocalcisome, *Mol. Biochem. Parasitol. 114*, 151−159.
6. Seufferheld, M., Vieira, M. C., Ruiz, F. A., Rodrigues, C. O., Moreno, S. N., and Docampo, R. (2003) Identification of organelles in bacteria similar to acidocalcisomes of unicellular eukaryotes, *J. Biol. Chem. 278*, 29971−29978.
7. Rea, P. A., Kim, Y., Sarafian, V., Poole, R. J., Davies, J. M., and Sanders, D. (1992) Vacuolar H^+-translocating pyrophosphatases: a new category of ion translocase, *Trends Biochem. Sci. 17*, 348−353.
8. Nyrén, P., Nore, B. F., and Strid, Å. (1991) Proton-pumping *N*,*N*′-dicyclohexylcarbodiimide-sensitive inorganic pyrophosphate synthase from *Rhodospirillum rubrum*: purification, characterization, and reconstitution, *Biochemistry 30*, 2883−2887.
9. Sato, M. H., Kasahara, M., Ishii, N., Homareda, H., Matsui, H., and Yoshida, M. (1994) Purified vacuolar inorganic pyrophosphatase consisting of a 75-kDa polypeptide can pump H^+ into reconstituted proteoliposomes, *J. Biol. Chem. 269*, 6725−6728.
10. Kim, E. J., Zhen, R. G., and Rea, P. A. (1994) Heterologous expression of plant vacuolar pyrophosphatase in yeast demonstrates sufficiency of the substrate-binding subunit for proton transport, *Proc. Natl. Acad. Sci. U.S.A. 91*, 6128−6132.
11. Sato, M. H., Maeshima, M., Ohsumi, Y., and Yoshida, M. (1991) Dimeric structure of H^+-translocating pyrophosphatase from pumpkin vacuolar membranes, *FEBS Lett. 290*, 177−180.
12. Wu, J. J., Ma, J. T., and Pan, R. L. (1991) Functional size analysis of pyrophosphatase from *Rhodospirillum rubrum* determined by radiation inactivation, *FEBS Lett. 283*, 57−60.
13. Davies, J. M., Rea, P. A., and Sanders, D. (1991) Vacuolar proton-pumping pyrophosphatase in *Beta vulgaris* shows vectorial activation by potassium, *FEBS Lett. 278*, 66−68.
14. Pérez-Castiñeira, J. R., Lopez-Marques, R. L., Losada, M., and Serrano, A. (2001) A thermostable K^+-stimulated vacuolar-type pyrophosphatase from the hyperthermophilic bacterium *Thermotoga maritima*, *FEBS Lett. 496*, 6−11.
15. Belogurov, G. A., and Lahti, R. (2002) A lysine substitute for K^+. A460K mutation eliminates K^+ dependence in H^+-pyrophosphatase of *Carboxydothermus hydrogenoformans*, *J. Biol. Chem. 277*, 49651−49654.
16. Davies, J. M., Poole, R. J., Rea, P. A., and Sanders, D. (1992) Potassium transport into plant vacuoles energized directly by a proton-pumping inorganic pyrophosphatase, *Proc. Natl. Acad. Sci. U.S.A. 89*, 11701−11705.
17. Ros, R., Romieu, C., Gibrat, R., and Grignon, C. (1995) The plant inorganic pyrophosphatase does not transport K^+ in vacuole membrane vesicles multilabeled with fluorescent probes for H^+, K^+, and membrane potential, *J. Biol. Chem. 270*, 4368−4374.
18. Nelson, K. E., Clayton, R. A., Gill, S. R., Gwinn, M. L., Dodson, R. J., Haft, D. H., Hickey, E. K., Peterson, J. D., Nelson, W. C., Ketchum, K. A., McDonald, L., Utterback, T. R., Malek, J. A., Linher, K. D., Garrett, M. M., Stewart, A. M., Cotton, M. D., Pratt, M. S., Phillips, C. A., Richardson, D., Heidelberg, J., Sutton, G. G., Fleischmann, R. D., Eisen, J. A., Fraser, C. M., and et al. (1999) Evidence for lateral gene transfer between Archaea and bacteria from genome sequence of *Thermotoga maritima*, *Nature 399*, 323−329.
19. Stemmer, W. P., and Morris, S. K. (1992) Enzymatic inverse PCR: a restriction site independent, single-fragment method for high-efficiency, site-directed mutagenesis, *Biotechniques 13*, 214−220.
20. Miroux, B., and Walker, J. E. (1996) Over-production of proteins in *Escherichia coli*: mutant hosts that allow synthesis of some membrane proteins and globular proteins at high levels, *J. Mol. Biol. 260*, 289−298.
21. Childers, S. E., Vargas, M., and Noll, M. K. (1992) Improved methods for cultivation of the extremely thermophilic bacterium *Thermotoga neapolitana*, *Appl. Environ. Microbiol. 58*, 3949−3953.
22. Baykov, A. A., and Avaeva, S. M. (1981) A simple and sensitive apparatus for continuous monitoring of orthophosphate in the presence of acid-labile compounds, *Anal. Biochem. 116*, 1−4.
23. Nýren, P., and Lundin, A. (1985) Enzymatic method for continuous monitoring of inorganic pyrophosphate synthesis, *Anal. Biochem. 151*, 504−509.
24. Fabrichniy, I. P., Kasho, V. N., Hyytiä, T., Salminen, T., Halonen, P., Dudarenkov, V. Yu., Heikinheimo, P., Chernyak, V. Ya., Goldman, A., Lahti, R., Cooperman, B. S., and Baykov, A. A. (1997) Structural and functional consequences of substitutions at the tyrosine 55-lysine 104 hydrogen bond in *Escherichia coli* inorganic pyrophosphatase, *Biochemistry 36*, 7746−7753.
25. Zyryanov, A. B., Vener, A. V., Salminen, A., Goldman, A., Lahti, R., and Baykov, A. A. (2004) Rates of elementary catalytic steps for different metal forms of the family II pyrophosphatase from *Streptococcus gordonii*, *Biochemistry 43*, 1065−1074.
26. Laemmli, U. K. (1970) Cleavage of structural proteins during the assembly of the head of bacteriophage T4, *Nature 227*, 680−685.
27. Bradford, M. M. (1976) A rapid and sensitive method for the quantitation of microgram quantities of protein utilizing the principle of protein-dye binding, *Anal. Biochem. 72*, 248−254.
28. Belogurov, G. A., Turkina, M. V., Penttinen, A., Huopalahti, S., Baykov, A. A., and Lahti, R. (2002) H^+-pyrophosphatase of *Rhodospirillum rubrum*. High yield expression in *Escherichia coli* and identification of the Cys residues responsible for inactivation my mersalyl, *J. Biol. Chem. 277*, 22209−22214.

29. Baykov, A. A., Dubnova, E. B., Bakuleva, N. P., Evtushenko, O. A., Zhen, R. G., and Rea, P. A. (1993) Differential sensitivity of membrane-associated pyrophosphatases to inhibition by diphosphonates and fluoride delineates two classes of enzyme, *FEBS Lett. 327*, 199−202.
30. Tusnady, G. E., and Simon, I. (1998) Principles governing amino acid composition of integral membrane proteins: application to topology prediction, *J. Mol. Biol. 283*, 489−506.
31. Mimura, H., Nakanishi, Y., Hirono, M., and Maeshima, M. (2004) Membrane topology of the H^+-pyrophosphatase of *Streptomyces coelicolor* determined by cysteine-scanning mutagenesis. *J. Biol. Chem. 279*, 35106−35112.
32. Daley, L. A., Renosto, F., and Segel, I. H. (1986) ATP sulfurylase-dependent assays for inorganic pyrophosphate: applications to determining the equilibrium constant and reverse direction kinetics of the pyrophosphatase reaction, magnesium binding to orthophosphate, and unknown concentrations of pyrophosphate, *Anal. Biochem. 157*, 385−395.
33. Flodgaard, H., and Fleron, P. (1974) Thermodynamic parameters for the hydrolysis of inorganic pyrophosphate at pH 7.4 as a function of Mg^{2+}, K^+, and ionic strength determined from equilibrium studies of the reaction, *J. Biol. Chem. 249*, 3465−3474.
34. Baykov, A. A., Shestakov, A. S., Kasho, V. N., Vener, A. V., and Ivanov, A. H. (1990) Kinetics and thermodynamics of catalysis by the inorganic pyrophosphatase of *Escherichia coli* in both directions, *Eur. J. Biochem. 194*, 879−887.
35. Smirnova, I. N., Kasho, V. N., Volk, S. E., Ivanov, A. H., and Baykov, A. A. (1995) Rates of elementary steps catalyzed by rat liver cytosolic and mitochondrial inorganic pyrophosphatases in both directions, *Arch. Biochem. Biophys. 318*, 340−348.
36. Hackney, D. D. (1980) Theoretical analysis of distribution of $[^{18}O]P_i$ species during exchange with water. Application to exchanges catalyzed by yeast inorganic pyrophosphatase, *J. Biol. Chem. 255*, 5320−5328.
37. Harvey, G. W., and Keister, D. L. (1981) Energy-linked reactions in photosynthetic bacteria: $P_i \leftrightarrows HOH$ oxygen exchange catalyzed by the membrane-bound inorganic pyrophosphatase of *Rhodospirillum rubrum*, *Arch. Biochem. Biophys. 208*, 426−430.
38. Baykov, A. A., Kasho, V. N., Bakuleva, N. P., and Rea P. A. (1994) Oxygen exchange reactions catalyzed by vacuolar H^+-translocating pyrophosphatase, *FEBS Lett. 350*, 323−327.
39. Huber, R., Langworthy, T. A., König, H., Thomm, M., Woese, C. R., Sleytr, U. B., and Stetter, K. O. (1986) *Thermotoga maritima* sp. nov. represents a new genus of unique extremely thermophilic eubacteria growing up to 90 °C, *Arch. Microbiol. 144*, 324−333.
40. Castle, A. M., Macnab, R. M., and Shulman, R. G. (1986) Measurement of intracellular sodium concentration and sodium transport in *Escherichia coli* by ^{23}Na nuclear magnetic resonance, *J. Biol. Chem. 261*, 3288−3294.
41. Delort, A. M., Dauphin, G., Guyot, J., and Jeminet, G. (1989) Study by NMR of the mode of action of monensin on *Streptococcus faecalis* de-energized and energized cells, *Biochim. Biophys. Acta 1013*, 11−20.
42. Gilboa, H., Kogut, M., Chalamish, S., Regev, R., Avi-Dor, Y., and Russell, N. J. (1991) Use of ^{23}Na nuclear magnetic resonance spectroscopy to determine the true intracellular concentration of free sodium in a halophilic eubacterium, *J. Bacteriol. 173*, 7021−7023.
43. Nagata, S., Adachi, K., Shirai, K., and Sano, H. (1995) ^{23}Na NMR spectroscopy of free Na^+ in the halotolerant bacterium *Brevibacterium* sp. and *Escherichia coli*, *Microbiology 141*, 729−736.
44. Schwaab, V., Matheron, C., Delort, A. M., Gaudet, G., and Forano, E. (2001) In vivo ^{23}Na nuclear magnetic resonance study of maintenance of a sodium gradient in the ruminal bacterium *Fibrobacter succinogenes* S85, *Appl. Environ. Microbiol. 67*, 4390−4392.

BI048429G